

## Free convection modeling over a vertical flat plate embedded in saturated porous medium with a variable heat source and radiation flux

Driss Achemlal<sup>1\*</sup>, Mohammed Sriti<sup>1</sup>, Mohamed El Haroui<sup>1</sup>, Mohammed Guedda<sup>2</sup>

<sup>1</sup> University of Sidi Mohamed Ben Abdellah, Polydisciplinary Faculty of Taza, Taza BP.1223, Morocco

<sup>2</sup> University of Picardie Jules-Verne, Faculty of Mathematics and computer Science, Rue Saint-Leu 80039, Amiens, France

(Received December 15 2012, Revised May 09 2013, Accepted July 01 2013)

**Abstract.** The main objective of this paper is to study the effect of thermal radiation on the boundary layer convection flow along a vertical plate embedded in saturated porous medium with an internal heat source. The temperature distribution of the plate has been assumed as  $T_w = T_\infty + Ax^\lambda$  and subjected to an applied lateral mass flux proportional to  $x^{\frac{\lambda-1}{2}}$  quantity, where  $x$  is the distance measured along the vertical plate and  $\lambda$  is the constant temperature exponent. Several similarity solutions were obtained according to the exponent parameter, but only three physical cases were studied :  $\lambda = 0, 1/3$  and  $1$  which correspond to isothermal plate, uniform surface heat flux and linear temperature distribution with uniform lateral mass flux at the plate, respectively. The non-linear equation of the similarity analysis with the boundary layer conditions has been solved numerically using a fifth-order Runge-Kutta scheme coupled with the shooting method. Also, the effect of the governing physical parameters on velocity and temperature, shear stress, Nusselt number and boundary layer thickness profiles have been computed and studied with help of graphs.

**Keywords:** free convection, saturated porous medium, suction/injection, thermal radiation

### 1 Introduction

Convective flow through porous media is a branch of research undergoing rapid growth in fluid mechanics and heat transfer. This is quite natural because of its important applications in chemical engineering, soil physics, nuclear reactors, oil extraction, transport processes in aquifers, biological systems and many others. The growing volume of work devoted to this area is amply documented in the recent excellent reviews in [6, 8, 12].

In certain porous media applications such as those involving heat removal from nuclear fuel debris, underground disposal of radioactive waste material, storage of food stuffs and exothermic chemical reactions, the influence of fluid heat generation is important. A simulation of such situations requires the addition of a heat source term in the energy equation<sup>[9]</sup>. In most cases, this term is assumed constant or temperature dependent. Radiation effects on free convection flow are important in the context of space technology and processes involving high temperatures, such as: glass manufacturing, furnace technology, high temperature aerodynamics and fire dynamics.

Many studies have appeared concerning the interaction of radiative flux with thermal convection flows. In view of this, Hossain and Pop [5] have analysed the radiation effect on a free convection flow along an inclined plate in a porous space. Raptis [10] has considered thermal radiation and free convection in a porous space. Ghosh and Bég [3] have analysed theoretically the radiation effect on transient free convection heat transfer past a hot vertical surface in porous media. Cortell [2] has highlighted the effects of the internal heat generation and radiation on a certain free convection flow. Badruddin, Zainal et al. [1] studied the free

\* Corresponding author. E-mail address: driss.achemlal@yahoo.fr.

convection and radiation for a vertical wall with varying temperature embedded in a porous medium. Zuki et al. [11] have investigated numerically the free convection over a permeable horizontal flat plate embedded in a porous medium with the radiation effect and the mixed thermal boundary conditions. Mohamed et al. [7] discussed the combined radiation and free convection from a vertical wavy surface embedded in a porous medium. The effect of radiation on free convection over a vertical flat plate embedded in non-Newtonian fluid saturated porous medium has been studied in [4].

The objective of this paper is to study numerically, the similarity solutions of the problem which has physical applications using the fifth-order Runge-Kutta integration scheme coupled with the shooting iteration technique drawing the effects of various parameters involved in this study (see Table 1).

**Table 1.** Nomenclature

$A$	wall temperature parameter	$x$	coordinate along the plate
$a$	equivalent thermal diffusivity	$y$	coordinate normal to the plate
$B$	suction/injection velocity parameter	$\beta$	thermal expansion coefficient
$C_p$	specific heat of fluid	$\delta$	thickness of the boundary layer
$f$	dimensionless stream function	$\eta$	similarity variable
$f_w$	suction/injection parameter	$\theta$	dimensionless temperature
$g$	gravitational acceleration	$\lambda$	temperature exponent
$K$	permeability of the porous medium	$\nu$	kinematic viscosity
$K_t$	thermal conductivity of the porous medium	$\rho$	fluid density
$N_R$	thermal radiation parameter	$\sigma$	Stefan-Boltzman constant
$Nu_x$	local Nusselt number	$\chi$	mean absorption
$Q_r$	radiative heat flux	$\psi$	stream function
$Q_w$	local heat flux on the plate surface	$w$	wall plate condition
$Ra_x$	modified local Rayleigh number	$\infty$	infinity plate condition
$T$	fluid temperature	'	derivative with respect to $\eta$
$u$	velocity component in x direction		
$V_w$	lateral mass flux		
$v$	velocity component in y direction		

## 2 Mathematical analysis

The problem is to study the convection around a heated vertical flat plate embedded in a saturated porous medium in the presence of an internal heat source. The distribution of the plate temperature varies according to the relationship  $T_w = T_\infty + Ax^\lambda$ , where  $T_\infty$  is the temperature away from the plate assumed constant,  $A$  is a positive constant,  $\lambda$  is the exponent of the temperature supposed constant. Cartesian coordinates  $x$  and  $y$  are measured, respectively, along and perpendicular to the plate. It is assumed that the porous medium is isotropic and homogeneous, that all properties of the fluid and porous medium are constant, except the influence of density variation in the body force term, under the Boussinesq approximation. The convective fluid and the porous medium are in thermodynamic equilibrium anywhere. The flow is supposed two-dimensional, stationary and laminar for an incompressible fluid. The radiation heat flux in the x-direction is considered negligible in comparison to the y-direction. The coordinates system and the flow configuration are shown in Fig. 1.

Taking into account the above assumptions, the governing equations for the problem can be written as:

$$\frac{\partial u}{\partial x} + \frac{\partial v}{\partial y} = 0, \tag{1}$$

$$u = \frac{g\beta K}{\nu}(T - T_\infty), \tag{2}$$

$$u \frac{\partial T}{\partial x} + v \frac{\partial T}{\partial y} = a \frac{\partial^2 T}{\partial y^2} + \frac{\varphi}{\rho C_p} + \frac{1}{\rho C_p} \frac{\partial Q_r}{\partial y}. \tag{3}$$

The boundary conditions associated with the problem are:

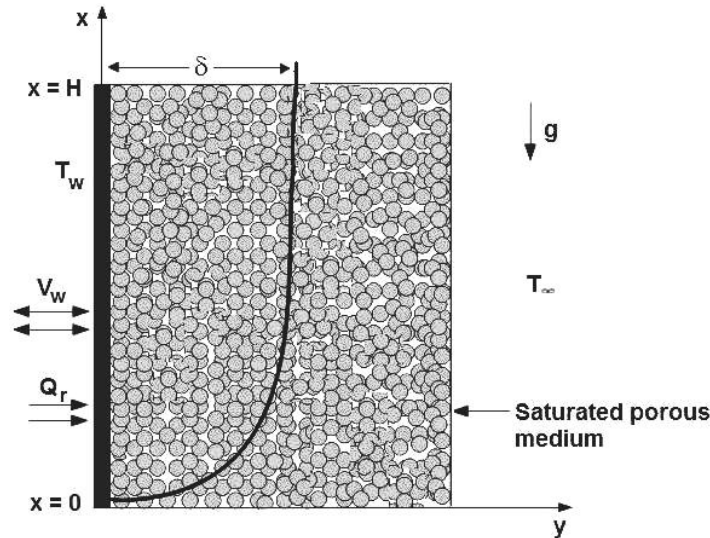


Fig. 1. Vertical flat plate in a saturated porous medium

$$y = 0 \quad x \geq 0, \quad v = V_w(x), \quad T = T_w(x), \tag{4}$$

$$y = \infty, \quad x \geq 0, \quad u = 0, \quad T = T_\infty, \tag{5}$$

where  $u$  and  $v$  are, respectively, the velocity components along  $x$  and  $y$  axes,  $T$  is the temperature of the fluid and  $\varphi$  is the internal source of heat. The constants  $\nu$ ,  $K$ ,  $a$ ,  $g$  and  $\rho$  are, respectively, kinematic viscosity, permeability, thermal diffusivity, gravitational acceleration and density.  $C_p$  and  $\beta$  are, respectively, the specific heat at a constant pressure and the coefficient of thermal expansion,  $V_w = Bx^{\frac{\lambda-1}{2}}$  is the lateral mass flux, where  $B$  is a constant.

The radiation flux on the basis of the Rosseland diffusion model for radiation heat transfer is expressed as:

$$Q_r = -\left(\frac{4\sigma}{3\chi}\right) \frac{\partial T^4}{\partial y}, \tag{6}$$

where  $\sigma$  is the Stefan–Boltzmann constant,  $\chi$  is the Rosseland mean absorption coefficient.

The temperature differences within the flow are assumed to be sufficiently small so that  $T^4$  may be expressed as linear function of the temperature. Hence, expanding  $T^4$  in a Taylor series about  $T_\infty$  and neglecting higher order terms.  $T^4$  can be expressed in the following way:

$$T^4 \approx 4 T_\infty^3 T - 3 T_\infty^4. \tag{7}$$

The non-linearity of our model and complexity of the phenomena encountered (boundary layer, instability, geometry of the porous medium, ...) make difficult its direct resolution. The transformation of the PDE system, describing the problem studied in a simple non-linear differential equation, then, becomes indispensable. To do this, we apply the similarity transformations, such as:

$$\eta(x, y) = \frac{y}{x} Ra_x^{1/2}, \tag{8}$$

$$\psi(x, y) = a Ra_x^{1/2} f(\eta), \tag{9}$$

$$\theta(\eta) = \frac{T - T_\infty}{T_w - T_\infty}, \tag{10}$$

$$Ra_x = \frac{g\beta K(T_w - T_\infty)x}{a\nu}, \tag{11}$$

$$\varphi = \rho C_p \frac{a(T_w - T_\infty) Ra_x}{x^2} e^{-\eta}, \tag{12}$$

where  $Ra_x$  is the Rayleigh number,  $\psi$  is the stream function defined by :  $u = \frac{\partial\psi}{\partial y}$  and  $v = -\frac{\partial\psi}{\partial x}$ .  $f$  and  $\theta$  are the dimensionless similarity functions.

Substitution in the governing Eqs. (1), (2) and (3) gives rise to the following system of ordinary differential equations:

$$f'(\eta) = \theta(\eta), \quad (13)$$

$$\left(1 + \frac{4}{3}N_R\right)\ddot{\theta}(\eta) - \lambda f'(\eta)\theta(\eta) + \frac{\lambda+1}{2}f(\eta)\dot{\theta}(\eta) + e^{-\eta} = 0, \quad (14)$$

$$\eta = 0, f(0) = f_w, f'(0) = 1, \theta(0) = 1, \quad (15)$$

$$\eta \rightarrow \infty, f'(\infty) = 0, \theta(\infty) = 0. \quad (16)$$

By injecting the Eq. (13) in (14), we obtain the non-linear differential Eq. (17) coupled with the boundary conditions (18) and (19).

$$\left(1 + \frac{4}{3}N_R\right)f'''(\eta) - \lambda f'^2(\eta) + \frac{\lambda+1}{2}f(\eta)f''(\eta) + e^{-\eta} = 0, \quad (17)$$

$$\eta = 0, f(0) = f_w, f'(0) = 1, \quad (18)$$

$$\eta \rightarrow \infty, f'(\infty) = 0, \quad (19)$$

where  $f_w = -\frac{2B}{\lambda+1} \left(\frac{\nu}{ag\beta KA}\right)^{1/2}$  is the suction/injection parameter,  $N_R = \frac{4\sigma T_\infty^3}{K_t\chi}$  is the radiation parameter.

The local heat flux on the surface of heated vertical plate is given by:

$$\begin{aligned} Q_w &= -K_t \left(\frac{\partial T}{\partial y}\right)_{y=0} + (Q_r)_w \\ &= -K_t A^{3/2} S^{1/2} x^{(3\lambda-1)/2} \theta'(0) \left(1 + \frac{4}{3}N_R\right), \end{aligned} \quad (20)$$

where  $S = \frac{g\beta K}{a\nu}$ ,  $\theta'(0)$  is the gradient of the temperature at the plate surface and  $K_t$  is the thermal conductivity.

The local Nusselt number is defined as:

$$Nu_x = -\theta'(0) \left(1 + \frac{4}{3}N_R\right) Ra_x^{1/2}. \quad (21)$$

Expression for shear stress  $\tau$  can be developed from the similarity solution:

$$\tau = \frac{\mu a}{x^2} Ra_x^{3/2} f''(\eta), \quad (22)$$

where  $f''(\eta)$  describes the dimensionless shear stress distribution in the boundary layer area and the particular value of  $f''(\eta)$  at  $\eta = 0$  represents the dimensionless shear stress on the plate surface.

The thickness of the thermal and dynamics boundary layer are equal and given by the equation:

$$\frac{\delta}{x} = \frac{\eta_T}{Ra_x^{1/2}}, \quad (23)$$

where  $\eta_T$  is the value of  $\eta$  at the edge of the boundary layer, conventionally defined as the place where  $\theta$  is equal to the value  $10^{-2}$ .

### 3 Numerical solution technique

The ordinary differential Eq. (17), governed by the boundary conditions (18) and (19), is non-linear. However, it is still difficult to solve it analytically. So, we have to rewrite it as a system of first-order differential equations. For this, we define the set as :  $\{g_1, g_2, g_3\} = \{f(\eta), f'(\eta), f''(\eta)\}$ .

So the non-linear differential Eq. (17) is equivalent to the system of differential equations of the first-order coupled with the boundary conditions:

$$g'_1 = g_2, \tag{24}$$

$$g'_2 = g_3, \tag{25}$$

$$g'_3 = \left( \frac{3}{3 + 4N_R} \right) \left( \lambda g_2^2 - \frac{\lambda + 1}{2} g_1 g_3 - e^{-\eta} \right), \tag{26}$$

$$\eta = 0, g_1 = f_w, g_2 = 1, \tag{27}$$

$$\eta \rightarrow \infty, g_2 = 0. \tag{28}$$

The system of differential Eqs. (24), (25) and (26) subjects to the boundary conditions (27) and (28) has been solved numerically by the fifth-order Runge-Kutta scheme, associated with the shooting method.

Since we have the initial conditions on  $g_1$  and  $g_2$ , it would be natural to seek the condition on  $g_3$  at  $\eta = 0$  ( $g_3(0)$ ). For given values of  $\lambda$  the value of  $g_3(0)$  is estimated and the differential Eqs. (24), (25) and (26) were integrated until the boundary condition at infinity,  $g_2(\eta)$  decay exponentially to 0. If the boundary condition at infinity is not satisfied, then, the numerical routine uses the calculated correction to the estimated value of  $g_3(0)$ . This process is repeated iteratively until exponentially decaying solution in  $g_2$  is obtained. A step size of  $\Delta\eta = 0.0001$  was found to be sufficient to give results that converge to within an error of  $10^{-6}$  in nearly all cases. The value of  $\eta_\infty$  was chosen as large as possible.

#### 4 Validation results

To assess the accuracy of our scheme, the comparisons are made with Postelnicu et al. [9] and Cortell [2] results in terms of  $f''(0)$  with various values of suction/injection parameter  $f_w$  and temperature exponent  $\lambda$ , presented in Tabs. 2 and 3. The obtained numerical results present no significant differences in Tab. 2 when the thermal radiation is absent for ( $\lambda = 1/3$ ). Although, in Tab. 3, all the values differences from R. Cortell [2] results are less than 1% when the thermal radiation is present for various values of suction/injection parameter  $f_w$  and temperature exponent parameter  $\lambda$ . Generally, the comparison shows a good agreement and also provides an excellent support of validity of our results. However, it could be said here with a positive note that the method used in this current model converges rapidly and accurate when compared to the method adopted by the previous work.

**Table 2.** Values of  $f$ ,  $f'$  and  $f''$  at the wall for  $\lambda = 1/3$  and  $f_w \neq 0$  when the thermal radiation is absent

$-f''(0) = -\theta'(0) = Nu_x Ra_x^{-1/2}$					
$\lambda$	$f(0) = f_w$	$f'(0)$	Postelnicu et al.	R. Cortell	Present Results
1/3	-1	1	-0.0662	-0.066178	-0.066291
	-0.6	1	-0.0094	-0.009357	-0.009433
	0.6	1	0.2869	0.286887	0.286969
	1	1	0.4289	0.428891	0.428903

#### 5 Results and discussion

The non-linear Eq. (17) subject to the boundary conditions (18) and (19) is solved numerically by using the fifth-order Runge-Kutta integration scheme associated with the shooting method. Similarity solutions are obtained for distinct values of the temperature exponent  $\lambda$  and suction/injection parameter  $f_w$ . However, only three physical solutions were selected for  $\lambda = 0, 1/3$  and 1 which correspond to isothermal plate, uniform surface heat flux and linear temperature distribution with uniform lateral mass flux at the plate, respectively.

**Table 3.** Values of  $f$  and  $f''$  at the wall for various values of  $\lambda$  and  $f_w$  when the thermal radiation is present

$$-f''(0) = -\theta'(0) = (Nu_x Ra_x^{-1/2}) / \left(1 + \frac{4}{3} N_R\right)$$

$\lambda$	$f(0) = f_w$	$N_R$	R. Cortell	Present Results
0	-0.1	1	-0.035835	-0.034408
1/3	-0.1	1	0.151726	0.152257
1/4	-0.1	1	0.111820	0.112474
	0	1	0.123578	0.124201
	1	1	0.135717	0.136312
1/5	-0.1	1	0.086099	0.086850
	0.1	1	0.109317	0.110004

The calculations were performed for different cases of the suction/injection parameter  $f_w$  which correspond to the suction ( $f_w > 0$ ), injection ( $f_w < 0$ ) and impermeable plate ( $f_w = 0$ ) in the presence of thermal radiation.

Numerical results for velocity  $f'(\eta)$  or temperature  $\theta(\eta)$  are illustrated in Figs. 2 ~ 7 for  $\lambda$ ,  $f_w$  and for selected values of the thermal radiation parameter  $N_R$ .

Fig. 2 shows that the magnitude of velocity and temperature profiles for an isothermal plate decrease with increasing  $N_R$  in the boundary layer area. But beyond the boundary layer, the profiles overlap and increase with the increasing of  $N_R$  for the case of the fluid injection. The decrease can be justified by the effect of the fluid injection (forced convection) that contributes to the reduction of temperature and velocity fields near the plate. The intersection point represents a balance between the effects of the fluid injection and thermal radiation. Away from the boundary layer, the fluid injection has no remarkable effect on the temperature and velocity fields when compared with the thermal radiation effect, which induces an increase of the velocity and temperature fields. From Fig. 3, we see that the velocity and temperature profiles for isothermal plate in the case of the fluid suction increase with the increase of  $N_R$ . Physically, this is explained by the effect of thermal radiation resulting in an increase in the buoyancy forces, which accelerates the flow convection along the plate.

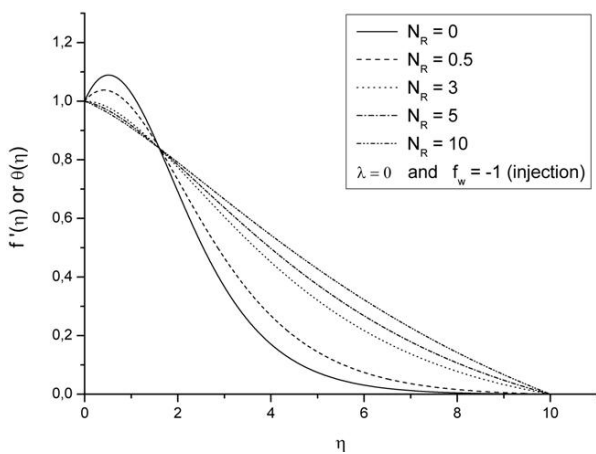


**Fig. 2.**  $f'$  or  $\theta$  versus  $\eta$  at  $\lambda = 0$  and  $f_w = -1$  for selected values of  $N_R$

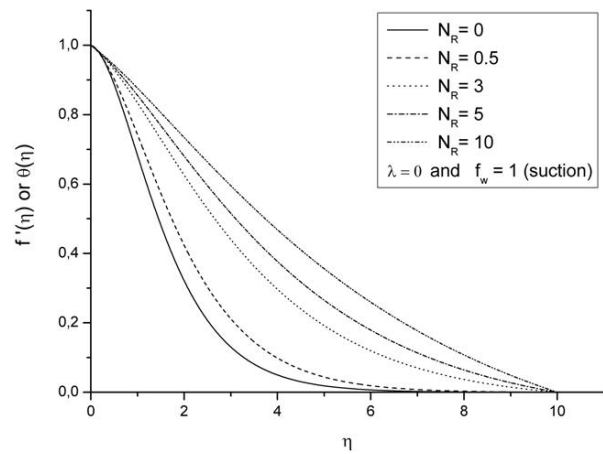


**Fig. 3.**  $f'$  or  $\theta$  versus  $\eta$  at  $\lambda = 0$  and  $f_w = 1$  for selected values of  $N_R$

Fig. 4 shows the dimensionless velocity and temperature profiles in the case of a uniform heat flux to the plate and for various values of  $N_R$  in the case of the fluid injection. It is seen, from this figure, that close to the plate, the velocity and temperature profiles decrease as  $N_R$  increases and away from the plate, the profiles increase with the increasing of  $N_R$ . These slight decreases which occur near the plate are due to the injection of the fluid with a uniform heat flux to the plate surface. Far from the plate, the effect of the fluid injection

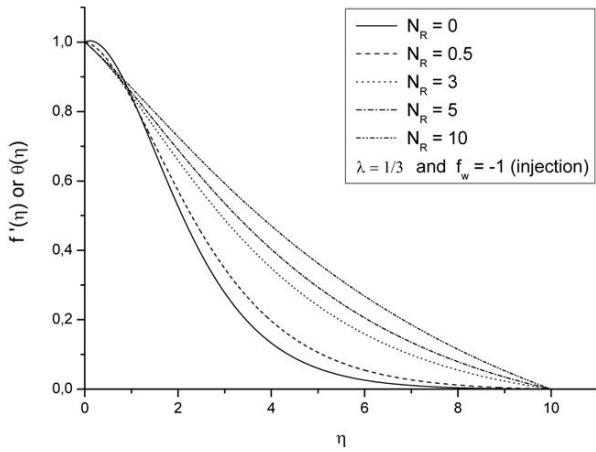


**Fig. 4.**  $f'$  or  $\theta$  versus  $\eta$  at  $\lambda = 1/3$  and  $f_w = -1$  for selected values of  $N_R$

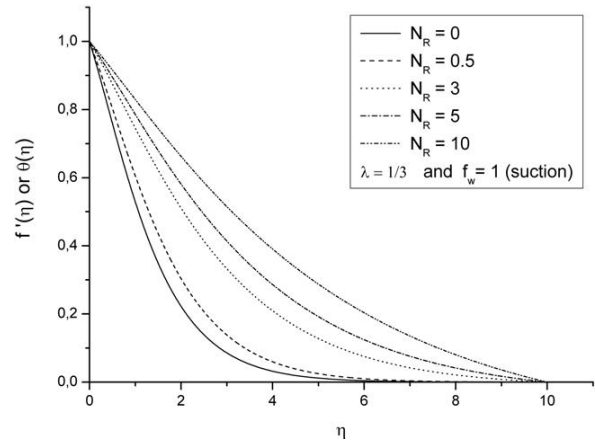


**Fig. 5.**  $f'$  or  $\theta$  versus  $\eta$  at  $\lambda = 1/3$  and  $f_w = 1$  for selected values of  $N_R$

is small compared to that of thermal radiation which encourages the process of the free convection and this justifies the growth of the velocity and temperature profiles.

The displayed Fig. 5 shows that, for a uniform heat flux to the plate in the case of the fluid suction, the velocity and temperature profiles increase with the increasing value of  $N_R$ . The increase observed from the surface of the plate can be explained by the insertion of the thermal radiation term in the energy equation. On the other hand, we observe a reduction in the temperature and velocity fields when compared with the case of the fluid injection (Fig. 4). This is due to the suction of the fluid at the plate.

In Figs. 6 and 7 the effect of the thermal radiation  $N_R$  on the velocity and temperature profiles in the case of a uniform lateral mass flux to the plate ( $V_w = B$ ) and a temperature that varies linearly with  $x$  in the cases  $f_w = -1$  and  $f_w = 1$  are shown. From these figures, it is observed that, as the interaction of the thermal radiation intensifies (increase in  $N_R$ ), the velocity and temperature increase with an accompanying increase in the velocity and temperature gradients at the wall. This is due to the high convection rate enriched by taking into account the thermal radiation flux coupled with the effect of a uniform lateral mass flux along the plate surface. We also see a remarkable reduction in the temperature and velocity profiles when compared with the case of the fluid injection (Fig. 6).

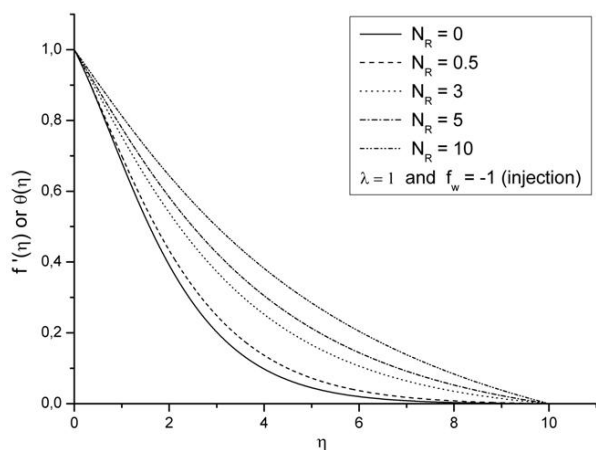


**Fig. 6.**  $f'$  or  $\theta$  versus  $\eta$  at  $\lambda = 1$  and  $f_w = -1$  for selected values of  $N_R$

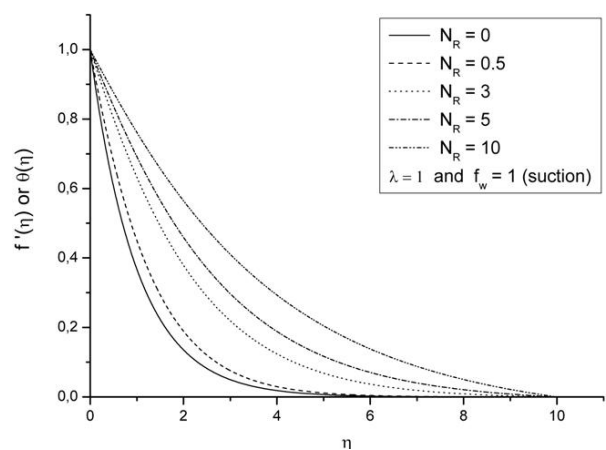


**Fig. 7.**  $f'$  or  $\theta$  versus  $\eta$  at  $\lambda = 1$  and  $f_w = 1$  for selected values of  $N_R$

Furthermore, the shear stress profiles shown, for an isothermal plate in the cases of the fluid injection and suction for various values of the thermal radiation parameter  $N_R$ , in Figs. 8 and 9 which indicate that

the minimum shear stress increases as  $N_R$  increases and this moves to the plate surface. It is deduced that the injection of the fluid through the plate contributes to a braking of the flow around the latter and consequently an increase of the minimum of frictional forces. Unlike the case of the suction of the fluid which simultaneously generates a decrease and a tendency of this minimum shear stress to the plate surface. Figs. 10 and 11 predict the influence of the radiation parameter  $N_R$  on the shear stress distributions for a uniform heat flux at the surface of the plate in the cases of the fluid injection and suction. The minimum shear stress increases with the increasing of  $N_R$  for  $f_w = -1$  and  $f_w = 1$  and this moves to the plate surface with the fluid suction.

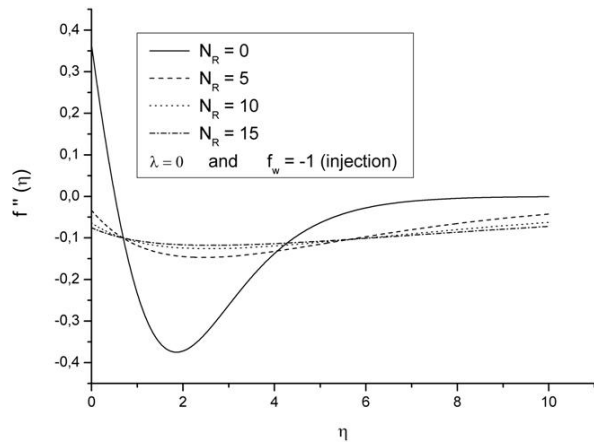


**Fig. 8.** Shear stress profiles for various values of  $N_R$ ,  $\lambda = 0$  and  $f_w = -1$

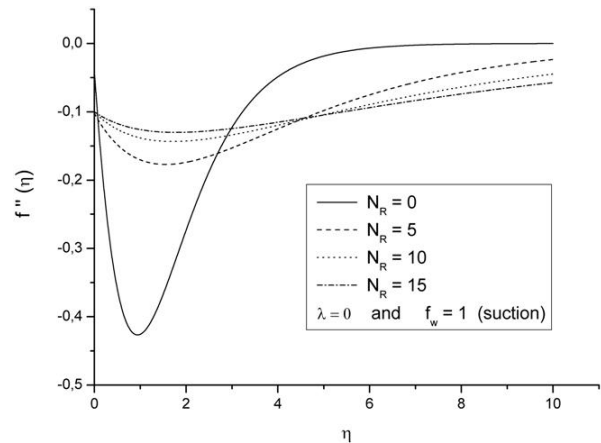


**Fig. 9.** Shear stress profiles for various values of  $N_R$ ,  $\lambda = 0$  and  $f_w = 1$

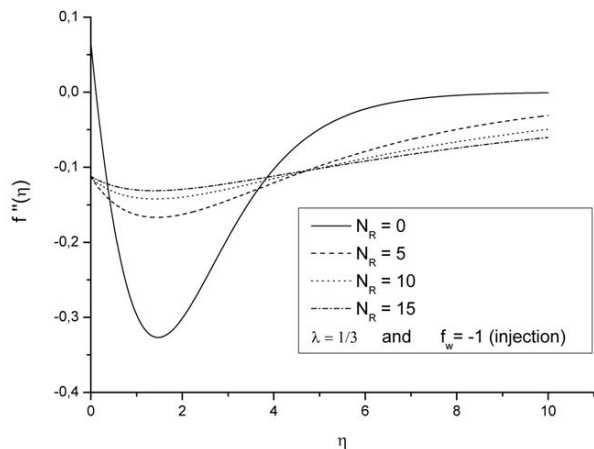


**Fig. 10.** Shear stress profiles for various values of  $N_R$ ,  $\lambda = 1/3$  and  $f_w = -1$

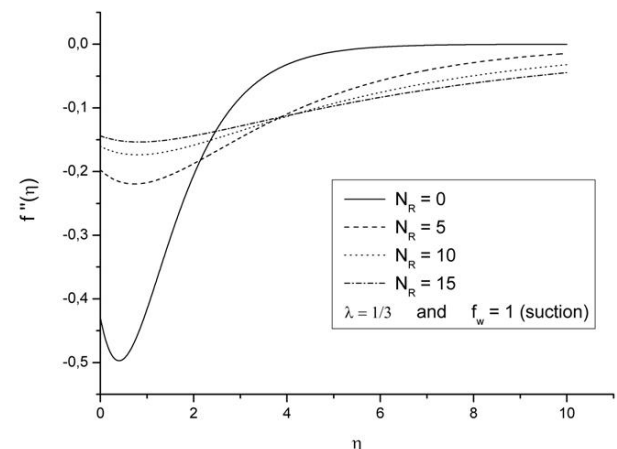


**Fig. 11.** Shear stress profiles for various values of  $N_R$ ,  $\lambda = 1/3$  and  $f_w = 1$

The influence of the thermal radiation parameter  $N_R$  on the shear stress profiles in the case of a uniform lateral mass flux to the plate ( $V_w = B$ ) for the fluid injection and suction is predicted in Figs. 12 and 13 which indicate a similar comportement of the minimum shear stress as that is cited in previous figures, except that in the case of the fluid suction, where the minimum shear stress is stucked with the plate surface.

Fig. 14 depicts the effect of varying the local thermal Rayleigh number on heat transfer for an impermeable and isothermal plate with a thermal radiation flux. It is observed that, for all the values of  $N_R$ , the heat transfer  $Nu$  increases with the increase in the intensity of the free convection flow, which clearly verifies the dependence of  $Nu_x$  and  $Ra_x^{1/2}$ .

The effect of the thermal radiation parameter  $N_R$  on the boundary layer thickness for an isothermal plate ( $\lambda = 0$ ) and for a uniform heat flux at the plate surface ( $\lambda = 1/3$ ), in the case of an impermeable plate, is shown in Figs. 15 and 16 respectively. It is observed that the boundary layer thickness increases with the



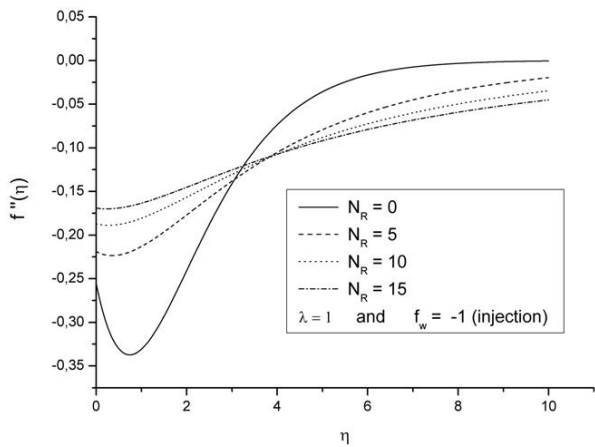


**Fig. 12.** Shear stress profiles for various values of  $N_R$ ,  $\lambda = 1$  and  $f_w = -1$

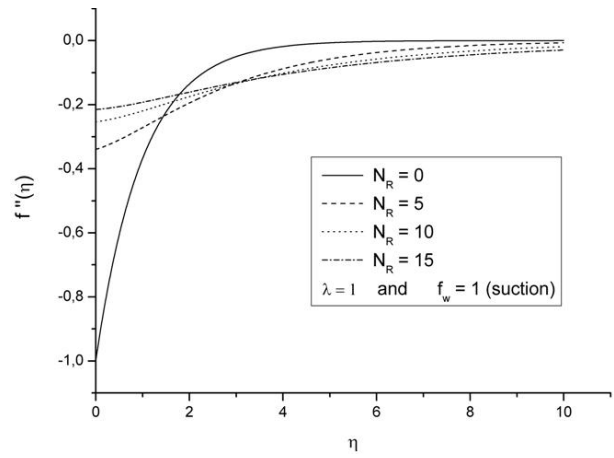


**Fig. 13.** Shear stress profiles for various values of  $N_R$ ,  $\lambda = 1$  and  $f_w = 1$

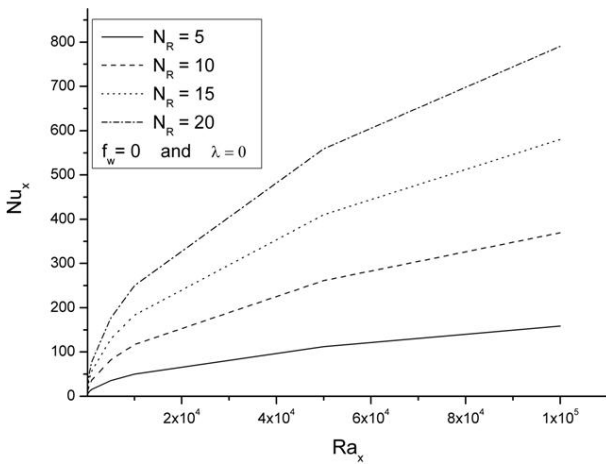


**Fig. 14.**  $Nu_x$  versus  $Ra_x$  at  $\lambda = 0$  and  $f_w = 0$  for various values of  $N_R$

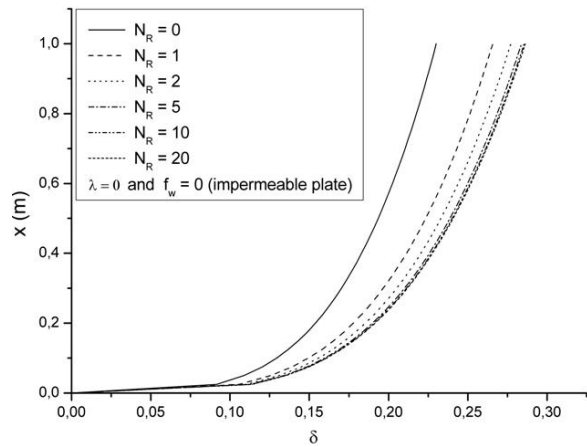


**Fig. 15.** Boundary layer thickness at  $\lambda = 0$  and  $f_w = 0$  for various values of  $N_R$

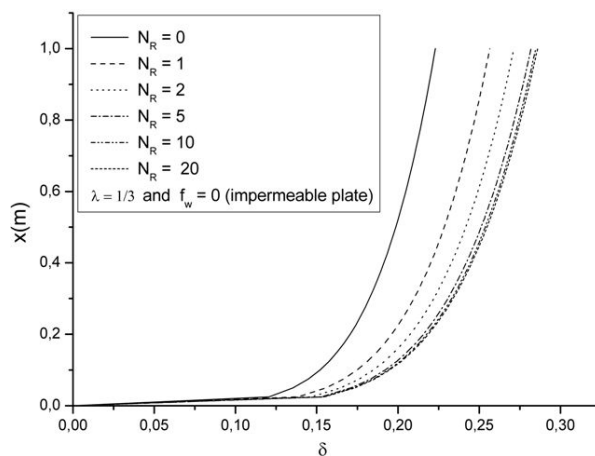


**Fig. 16.** Boundary layer thickness at  $\lambda = 1/3$  and  $f_w = 0$  for various values of  $N_R$

increase of the thermal radiation parameter, and it is clear that the larger values of this parameter has no significant influence on the boundary layer thickness.

## 6 Conclusion

In this paper, we have discussed the effects of the thermal radiation parameter, fluid suction/injection parameter and temperature exponent parameter on the free convection flow over a vertical flat plate embedded in a saturated porous medium with a variable internal heat source. The set of the equations governing the problem are reduced to ordinary differential equations with appropriate boundary conditions. Furthermore, the similarity equations are solved numerically by using the fifth-order Runge-Kutta scheme associated with the shooting method. The influence of the thermal radiation parameter  $N_R$ , the fluid suction/injection parameter  $f_w$  and the temperature exponent parameter  $\lambda$  on the velocity or temperature, the dimensionless shear stress, the Nusselt number and the boundary layer thickness profiles have been examined and discussed in details. From the present numerical investigation, we conclude that:

- The introduction of the thermal radiation in the study helps to intensify the heat transfer by convection.
- The fluid suction at the plate disadvantages the natural convection phenomenon at any point of the flow fields.
- The thermal radiation promotes the friction forces in the boundary layer and the minimum of these forces decreases and approaches the plate surface with the fluid suction.
- The heat transfer increases with the local Rayleigh number, and this increases becomes greater with the intensification of the thermal radiation.
- The thermal or dynamics boundary layer thickness increases with the increase of the thermal radiation parameter, and it is clear that the larger values of this parameter has no significant influence on the boundary layer thickness.

## References

- [1] I. Badruddin, Z. Zainal, et al. Free convection and radiation for a vertical wall with varying temperature embedded in a porous medium. *International journal of thermal sciences*, 2006, **45**(5): 487–493.
- [2] R. Cortell. Internal heat generation and radiation effects on a certain free convection flow. *International Journal of Nonlinear Science*, 2010, **9**(4): 468–469.
- [3] S. Ghosh, O. Béǵ. Theoretical analysis of radiative effects on transient free convection heat transfer past a hot vertical surface in porous media. *Nonlinear Analysis: Modelling and Control*, 2008, **13**(4): 419–432.
- [4] T. Grosan, I. Pop. The effect of radiation on free convection over a vertical flat plate embedded in non-newtonian fluid saturated porous medium. *International Journal of Applied Mechanics and Engineering*, 2006, **11**(3): 715–722.
- [5] M. Hossain, I. Pop. Radiation effect on darcy convection flow along an inclined surface placed in porous media. *Heat Mass Transfer*, 1997, **32**(4): 223–227.
- [6] M. Kaviany. *Principles of heat transfer in porous media*, 2nd edn. Springer Mechanical Engineering Series, New York - USA, 1995.
- [7] R. Mohamed, A. Mahdy, F. Hady. Combined radiation and free convection from a vertical wavy surface embedded in porous medium. *International Journal of Applied Mathematics and Mechanics*, 2008, **4**(1): 49–58.
- [8] D. Nield, A. Bejan. *Convection in porous media*, 3rd edn. Springer Science, New York - USA, 2006.
- [9] A. Postelnicu, T. Groşan, I. Pop. Free convection boundary-layer over a vertical permeable flat plate in a porous medium with internal heat generation. *International communications in heat and mass transfer*, 2000, **27**(5): 729–738.
- [10] A. Raptis. Radiation and free convection flow through a porous medium. *International communications in heat and mass transfer*, 1998, **25**: 289–295.
- [11] S. Zuki, M. Najihah, et al. Free convection over a permeable horizontal flat plate embedded in a porous medium with radiation effects and mixed thermal boundary conditions. *Journal of Mathematics and Statistics*, 2012, **8**(1): 122–128.
- [12] K. Vafai. *Handbook of porous media*, 2nd edn. CCR Press Taylor & Francis Group LLC, Boca Raton - USA, 2005.